

Modulation of Angiogenesis by a Tetrameric Tripeptide That Antagonizes Vascular Endothelial Growth Factor Receptor 1^{*[S]}

Received for publication, August 26, 2008, and in revised form, October 2, 2008. Published, JBC Papers in Press, October 15, 2008, DOI 10.1074/jbc.M806607200

Salvatore Ponticelli^{†1}, Daniela Marasco^{§1}, Valeria Tarallo[‡], Romulo J. C. Albuquerque^{¶12}, Stefania Mitola^{||}, Atsunobu Takeda^{¶13}, Jean-Marie Stassen^{**}, Marco Presta^{||}, Jayakrishna Ambati[¶], Menotti Ruvo^{§4}, and Sandro De Falco^{‡4,5}

From the [‡]Angiogenesis Laboratory and Stem Cell Fate Laboratory, Institute of Genetics and Biophysics “Adriano Buzzati-Traverso”, Consiglio Nazionale delle Ricerche (CNR), 80131 Napoli, Italy, the [§]Institute of Biostructures and Bioimaging, CNR, 80134 Napoli, Italy, the [¶]Department of Ophthalmology and Visual Sciences, University of Kentucky, Lexington, Kentucky 40536, the ^{||}Unit of General Pathology and Immunology, Department of Biomedical Sciences and Biotechnology, University of Brescia, 25123 Brescia, Italy, and ^{**}Thrombogenics, Campus Gasthuisberg, B-3000 Leuven, Belgium

Vascular endothelial growth factor receptor-1 (VEGFR-1, also known as Flt-1) is involved in complex biological processes often associated to severe pathological conditions like cancer, inflammation, and metastasis formation. Consequently, the search for antagonists of Flt-1 has recently gained a growing interest. Here we report the identification of a tetrameric tripeptide from a combinatorial peptide library built using non-natural amino acids, which binds Flt-1 and inhibits *in vitro* its interaction with placental growth factor (PlGF) and vascular endothelial growth factor (VEGF) A and B (IC₅₀ ~ 10 μM). The peptide is stable in serum for 7 days and prevents both Flt-1 phosphorylation and the capillary-like tube formation of human primary endothelial cells stimulated by PlGF or VEGF-A. Conversely, the identified peptide does not interfere in VEGF-induced VEGFR-2 activation. *In vivo*, this peptide inhibits VEGF-A- and PlGF-induced neoangiogenesis in the chicken embryo chorioallantoic membrane assay. In contrast, in the cornea, where avascularity is maintained by high levels of expression of the soluble form of Flt-1 receptor (sFlt-1) that prevents the VEGF-A activity, the peptide is able to stimulate corneal mouse neovascularization in physiological condition, as reported previously for others neutralizing anti-Flt-1 molecules. This tetrameric tripeptide represents a new, promising compound for therapeutic approaches in pathologies where Flt-1 activation plays a crucial role.

A complicated tuning of several growth factor families and related receptors regulates the formation of new vessels (1). Among these players, the activation of two vascular endothelial growth factor (VEGF)⁶ receptors, Flt-1 and VEGF receptor 2 (Flk-1 in mouse, KDR in human), represents a crucial event in both physiological and pathological angiogenesis (2–4). Three members of the VEGF family involved in angiogenesis bind and activate VEGF receptors; VEGF-A binds both Flt-1 and KDR receptors, whereas two other VEGF family members, VEGF-B and placental growth factor (PlGF), specifically bind Flt-1. The activity of VEGF-A is crucial both in physiological and in pathological angiogenesis, whereas that of PlGF and VEGF-B appears to be restricted to pathological conditions (5, 6).

Phenotype analysis of “knock out” mice and *in vivo* biochemical interaction studies strongly suggest that the inhibition of Flt-1 activity constitutes an alternative target for therapeutic modulation of angiogenesis as well as inflammatory disorders and metastatic process (7, 8). *Plgf* null mice (9), *Vegf-B* null mice (10), and mice engineered to express a truncated form of Flt-1 lacking the tyrosine kinase domain (11) are borne at Mendelian frequency and are healthy and fertile. However, pathological angiogenesis in the adult is impaired in all three mouse models. Moreover, Flt-1 blockade by neutralizing anti-Flt-1 monoclonal antibody (mAb) strongly reduces the neovascularization in tumors as well as in models of ischemic retinopathy and age-related macular degeneration (9, 12–14). Recently it has been reported that neutralizing mAb anti-PlGF is able to inhibit tumor angiogenesis with an efficacy comparable with that observed blocking VEGF/Flk-1 pathway (15).

In contrast to KDR, which is predominantly expressed by endothelial cells (ECs), expression of Flt-1 has been detected and functionally demonstrated also in smooth muscle cells (16), in monocyte-macrophage cells (17), and in bone marrow stem/

* This work was supported by AIRC (Associazione Italiana Ricerca sul Cancro, Grant 4840) and Telethon–Italy (Grant GGP08062) (to S. D. F.) and only in part by FIRB (Grant RBNE03PX83_005) (to M. R.) and National Institutes of Health (NIH) Grants EY015422, EY018350, and EY018836 (to J. A.). The costs of publication of this article were defrayed in part by the payment of page charges. This article must therefore be hereby marked “advertisement” in accordance with 18 U.S.C. Section 1734 solely to indicate this fact.

This manuscript is dedicated to the memory of Maria Graziella Persico, a wonderful scientist and woman who left us too early.

[S] The on-line version of this article (available at <http://www.jbc.org>) contains supplemental Experimental Procedures, three supplemental tables, and four supplemental figures.

¹ These authors equally contributed to this work.

² Supported by a Research to Prevent Blindness medical student fellowship and Fight for Sight.

³ Supported by Japan Society for the Promotion of Science for Young Scientists.

⁴ These authors are joint senior authors.

⁵ To whom correspondence should be addressed: Institute of Genetics and Biophysics “Adriano Buzzati-Traverso,” CNR, Via Pietro Castellino, 111, 80131 Naples, Italy. Tel.: 39-081-6132354; Fax: 39-081-6132595; E-mail: defalco@igb.cnr.it.

⁶ The abbreviations used are: VEGF, vascular endothelial growth factor; VEGFR-1 or -2, VEGF receptor 1 or 2; Flt-1, fms-related tyrosine kinase 1; sFlt-1, soluble Flt-1; PlGF, placental growth factor; Flk-1, fetal liver kinase receptor 1; KDR, kinase domain region; CTF, capillary-like tube formation; CAM, chorioallantoic membrane; CNV, corneal neovascularization; EC, endothelial cells; HUVEC, human umbilical vein endothelial cells; mAb, monoclonal antibody; ELISA, enzyme-linked immunosorbent assay; Fmoc, N-(9-fluorenyl)methoxycarbonyl; BSA, bovine serum albumin; PBS, phosphate-buffered saline; DMSO, dimethyl sulfoxide; HPLC, high pressure liquid chromatography.

progenitor-derived cells (12). The activation of Flt-1 is not only crucial for ECs stimulation during the neoangiogenesis process (18, 19) but also plays a fundamental role in the stabilization of neovessels through the recruitment of smooth muscle cells (16), in the recruitment and differentiation of monocyte-macrophage cells (17, 20–22) and, ultimately, in the reconstitution of hematopoiesis promoting the recruitment of Flt-1-positive cells from bone marrow microenvironment (23). Furthermore, Flt-1 activation is decisive in the recruitment of bone marrow-derived endothelial cells and hematopoietic precursors in tumor angiogenesis (12) as well as in inflammatory disorders (22). More recently, it has been shown that Flt-1-positive hematopoietic bone marrow progenitors are involved in the establishment of premetastatic niche and that an anti-Flt-1 mAb completely prevents metastatic process (24).

Flt-1 receptor also exists as an alternatively spliced soluble form (sFlt-1) (25) that represents one of the most potent physiological inhibitors of VEGFs activity. Indeed, it is expressed during embryonic development, where it regulates the availability of VEGF and, as recently reported, in the adults, it plays a pivotal role to maintain corneal avascularity (26).

Collectively, these data strongly indicate Flt-1 as an ideal target for fighting a number of major diseases (7). In the effort to identify new molecules able to selectively bind Flt-1 and neutralize its activity, we screened a random combinatorial tetrameric tripeptide library built using non-natural amino acids, using a competitive ELISA-based assay (27). The peptide mixtures composing the library were utilized as competitors of the PlGF/Flt-1 binding, and the most active component was isolated following an iterative process (28, 29). The biological activity of the selected peptide has then been assessed in several *in vitro* and *in vivo* assays demonstrating that it is a highly stable and selective Flt-1 binder able to suppress the receptor activation.

EXPERIMENTAL PROCEDURES

Synthesis of Combinatorial Tetrameric Tripeptide Library and Analogues of 4-23-5 Peptide—The peptide library was prepared using all commercially available amino acids and resins purchased from Chem-Impex International (Wood Dale, IL) and from Novabiochem (Laufelfingen, CH). As 30 different blocks were utilized (supplemental Table S1), a theoretical number of 27,000 peptides was generated, split in 30 separate pools of 900 peptides each. All residues were 9-fluorenylmethoxycarbonyl (Fmoc)-derivatized (>99%) and were utilized without any further purification. Amino acids in the D configuration and others bearing trifluoroacetic acid-stable side chain protections were chosen to increase the library chemical diversity and, at the same time, to introduce resistance to enzyme degradation (30) for *in vitro* and *in vivo* applications. The library was chemically synthesized following the Fmoc methodology (31), and sequence randomization was achieved applying the portioning-mixing process as reported elsewhere (28) (see also the supplemental Experimental Procedures). Other molecules, such as the monomeric, dimeric, and trimeric tripeptide variants, as well as the Ala-scanning peptides (where the monomers were systematically changed to alanine), were similarly prepared using suitable protecting groups. The cyclic dimeric variant was prepared as described elsewhere (29).

Iterative Deconvolution of Tetrameric Tripeptide Library—Recombinant PlGF, VEGF-A, VEGF-B, VEGFR-1/Fc chimera, VEGFR-2/Fc chimera of human and mouse origin, and normal or biotinylated antibodies anti-PlGF, anti-VEGF-A, and anti-VEGF-B were purchased from R&D Systems (Minneapolis, MN). At every step of the deconvolution process, peptide pools were tested with a molar excess of 1,000-fold (calculated on each single peptide) over PlGF (1.3×10^{-10} M). Following the identification of active pools, dose-dependent inhibition experiments using 500-, 1,000-, 1,500-, and 2,000-fold excess were performed to confirm the inhibitory capacity. The first active pool identified was the 4-X-X (X indicates randomized positions) where “4” identified the amino acid D-glutamic acid (D-Glu, supplemental Table S1). This pool was resynthesized in 30 subpools each composed of 30 peptides and submitted to the second screening round that allowed the identification of the subpool 23 (4-23-X). The number “23” identified the amino acid L-cysteine(S-benzyl) (supplemental Table S1). Finally, the 30 single peptides composing the 4-23-X pool were synthesized and submitted to the final screening. The peptide 4-23-5, where the number “5” identified the amino acid L-cyclohexylalanine (supplemental Table S1), was the unique molecule showing inhibitory activity.

ELISA-based Assays—The competitive ELISA-based assay (27) for the screening of the peptide library and for dose-dependent experiments was performed by coating on 96-well plates a recombinant form of Fc/Flt-1 at 0.5 μ g/ml, 100 μ l/well (the same volume was used for all subsequent steps), 16 h at room temperature. The plate was then blocked for 3 h at room temperature with 1% bovine serum albumin (BSA), and a recombinant form of PlGF at 5 ng/ml concentration in PBS containing 0.1% BSA, 5 mM EDTA, 0.004% Tween 20 (PBET) was added and incubated for 1 h at 37 °C followed by 1 h at room temperature. A biotinylated anti-human PlGF polyclonal antibody diluted in PBET at 300 ng/ml was added to the wells and incubated for 1 h at 37 °C followed by 1 h at room temperature. A solution containing an avidin and biotinylated horseradish peroxidase macromolecular complex was prepared as suggested by the manufacturer (Vectastain *elite* ABC kit, Vector Laboratories, Burlingame, CA) and added to the wells and incubated for 1 h at room temperature followed by the horseradish peroxidase substrate composed of 1 mg/ml *ortho*-phenylenediamine in 50 mM citrate phosphate buffer, pH 5, 0.006% of H₂O₂, incubated for 40 min in the dark at room temperature. The reaction was blocked by adding 30 μ l/well of 4 N H₂SO₄, and the absorbance was measured at 490 nm on a microplate reader (BenchMark, Bio-Rad). Peptide pools or single peptides dissolved in DMSO were properly diluted and added to the wells along with ligand. For dose-dependent experiments performed with VEGF-A and VEGF-B, 10 ng/ml recombinant proteins and 500 ng/ml polyclonal antibody, anti-human VEGF-A or anti-human VEGF-B, were used. 4-23-5 and control peptides were used at concentrations ranging between 1.56 and 50.0 μ M. Using the same ELISA-based assay, the inhibitory capacities of alanine-scan peptides and structurally related analogues (supplemental Table S3) were investigated in both PlGF and VEGF interaction with Flt-1 receptor. Analogues were used at 50 μ M, whereas the 4-23-5 peptide was used at 12.5 μ M. To evaluate the

Anti-VEGFR-1 Peptide Modulates Angiogenesis

binding of the 4-23-5 peptide to Flt-1 receptor, the peptide or the negative controls were coated at 20 μM for 16 h at 4 °C. A recombinant form of extracellular domains of human and mouse Flt-1 receptors fused to human Fc in PBET was added to the wells and incubated for 1 h at 37 °C followed by 30 min at room temperature. Goat anti-human Fc antibody (Jackson ImmunoResearch, West Grove, PA) and the secondary donkey anti-goat hypoxanthine-guanine phosphoribosyltransferase antibody (Santa Cruz Biotechnology, Santa Cruz, CA), both at 1:1000 dilution, were added and incubated for 1 h at room temperature. Finally, plates were developed as described above. To evaluate the binding of 4-23-5 to VEGFR-2, recombinant human Fc/KDR and mouse Fc/Flk-1 were used. To evaluate the ability of PlGF and VEGF-A to compete the interaction of Flt-1 with the synthetic ligand, 4-23-5 was coated at 20 μM , and the human Fc/Flt-1 receptor was used at a fixed concentration (125 pM). The dose-dependent competition was performed using PlGF and VEGF-A at concentrations ranging between 0.05 and 6.25 nM.

Stability Assay—The selected 4-23-5 peptide was dissolved in neat DMSO at a 10 mg/ml concentration. The sample was then serially diluted in PBS, pH 7.3, containing 10% fetal calf serum to obtain 100 $\mu\text{g}/\text{ml}$ solutions and incubated at 37 °C for 168 h. 10- μl aliquots (1.0 μg of total peptide) were removed after every hour within the first 12 h and subsequently at 24, 72, 120, and 168 h. Samples were immediately centrifuged for 5 min at 14,000 rpm and analyzed by reverse phase-HPLC after discarding the pellet. To closely check the peptide concentration within samples, a reference curve was obtained by analyzing, under the same conditions, different amounts of the pure compound dissolved in DMSO (the peptide solubility in DMSO is >100 mg/ml). The reference curve was also used to exclude effects of sample subtraction by nonspecific binding to albumin or other serum proteins. The experiment was carried out in duplicate, and the data were reported as residual peptide in solution (in percentages) *versus* time.

Inhibition of Flt-1 Phosphorylation and Capillary-like Tube Formation—These assays were performed as described elsewhere (18). In phosphorylation experiments, to induce Flt-1 and KDR receptor activation, 20 ng/ml PlGF and 50 ng/ml VEGF were used on starved 293-Flt-1 or HUVEC cells. To detect phosphorylated forms of receptors in Western blot experiments, anti-pFlt-1 (R&D Systems) at 1:500 dilution and anti-pKDR (Cell Signaling, Danvers, MA) at 1:1000 dilution antibodies were used.

Capillary-like tube formation were performed in 24-well culture plates. At the end of the experiment, the culture medium was replaced with PBS, and the images were captured with the inverted microscope Leica DM IRB (Wetzlar, Germany) equipped with a Leica DC 350 FX camera (original magnification $\times 10$). Images were acquired with Leica FW 4000 software.

Chicken Embryo Chorioallantoic Membrane (CAM) Assay—Alginate beads (5 μl) containing vehicle, 150 ng/embryo of VEGF-A, or 250 ng/embryo of PlGF with or without peptides (0.25 and 0.025 nmol/embryo) were prepared as described previously (32) and placed on top of the CAM of fertilized White Leghorn chicken eggs at day 11 of incubation (6–8 eggs per experimental group). After 72 h, new blood vessels converging

toward the implant were counted by two observers in a double-blind fashion under a stereomicroscope and photographed *in ovo* at original magnification $\times 5$, using a STEMI SR stereomicroscope, equipped with an objective *f* equal to 100 mm with adapter ring 475070 (Zeiss, Germany) and a Camedia C-4040 digital camera (Olympus, Melville, NY). Images were acquired and processed using the Image-Pro Plus software. Differences among groups were tested by one-way analysis of variance using the SPSS statistical package (version 12.1, Chicago, IL).

Cornea Neovascularization (CNV)—Single injections (33-gauge needle) of 0.40, 4.0, or 20 nmol of peptide 4-23-5 and of only 20 nmol of control peptide in the same volume of DMSO were carried out in the corneas of BALB/c mice ($n = 3$ each group). Eyes were harvested 7 days after injection, corneas were gently isolated, and immunohistochemical staining for endothelial cells was performed. Corneas were fixed in 100% acetone for 20 min, washed with PBS, 0.05% Tween 20 for 10 min four consecutive times, and blocked with 3% BSA in PBS for 48 h. The corneas were then incubated with fluorescein isothiocyanate-coupled monoclonal anti-mouse CD31 antibody (Pharmingen) at 3:1000 and rabbit anti-mouse LYVE-1 antibody (Abcam, Cambridge, UK) at 3:1000 in 3% BSA PBS solution at 4 °C for 48 h. The corneas were washed as described previously and incubated in Cy3-conjugated donkey anti-rabbit at 3:1000 in 3% BSA PBS solution for 2 h, after which they were washed and mounted with an antifading agent (Vectashield, Vector Laboratories). The corneal flat mounts were visualized with a fluorescent microscope (Nikon Eclipse TE2000-E) equipped with Nikon DXM200F camera at original magnification $\times 4$. Images acquisitions were performed with Nikon, ACT-1 software, version 2.63. Blood vessels were identified as CD31-positive and LYVE-1-negative.

RESULTS

Synthesis, Characterization, and Screening of the Combinatorial Peptide Library—To increase the molecular surface, the library was assembled as described previously (28) on a peptide scaffold composed by a polylysine core (supplemental Fig. S1) (33). To obtain mixtures, three levels of randomization were achieved applying the portioning-mixing method (34, 35). The tetrameric library was synthesized using 29 non-natural amino acids plus glycine (supplemental Table S1) and was initially arranged in 30 pools, each identified with the N-terminal building block. Each pool contained 900 different molecules (30^2). The total complexity of the library was instead determined by the formula $30^3 = 27,000$ different peptides.

Peptide mixtures were obtained in high yield (about 70%) as calculated assuming an average molecular mass of 2130 atomic mass units for each library component and with an average purity of the crude products >85% (as determined on the single molecules assayed during the last screening round, not shown). The liquid chromatography-mass spectrometry analyses of some selected 30-component mixtures showed that the expected molecules were almost all equally represented and that molecular weights were in very good agreement with those calculated (not shown). Liquid chromatography-mass spectrometry analyses of single peptides also showed very good

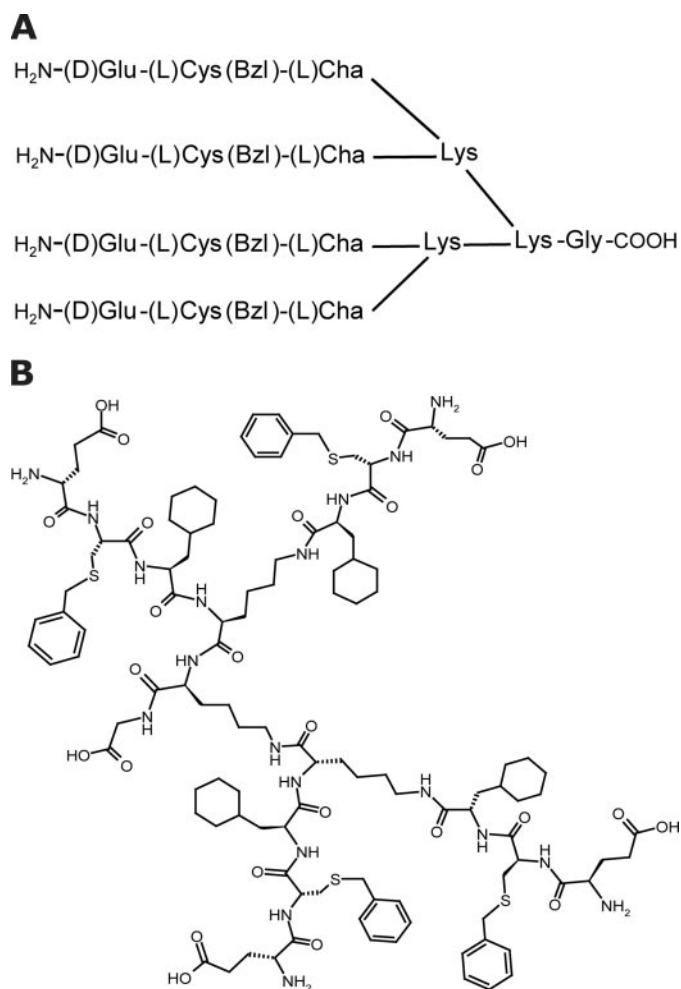


FIGURE 1. **Structure of 4-23-5 peptide.** *A*, schematic representation of the 4-23-5 tetrameric tripeptide. *L*-Cys(Bzl), *L*-cysteine(*S*-benzyl); *L*-Cha, *L*-cyclohexylalanine. *B*, chemical structure of the 4-23-5 peptide that has a calculated MW of 2362.02 atomic mass units.

agreement between calculated and experimental molecular weights (supplemental Table S2).

The screening was carried out by a competition assay, whereby the displacement of soluble recombinant PlGF from coated Flt-1 by the peptide pools was evaluated. PlGF was used in the assay as, among all the VEGF family members, it shows the highest affinity for Flt-1 (6). The iterative procedure consisted of three screening rounds that led to the selection of building blocks denoted as 4, 23, and 5 in positions 1, 2, and 3, respectively (supplemental Table S1). A schematic representation and the chemical structure of the selected tetrameric tripeptide, hereafter named 4-23-5, are reported in Fig. 1. Monomers 4, 23, and 5 refer to the amino acids *D*-glutamic acid (*D*-Glu), *S*-benzylated *L*-cysteine, and *L*-cyclohexylalanine.

The selected peptide was readily resynthesized on a larger scale and purified by reverse phase HPLC. In the same ELISA assay, the purified 4-23-5 blocked the interaction of human PlGF with Flt-1 in a dose-dependent manner, with an IC₅₀ of about 10 μM (Fig. 2A), whereas the control tetrameric peptides 21-1-5 and 4-23-A (supplemental Table S3) did not show any effect (Fig. 2A).

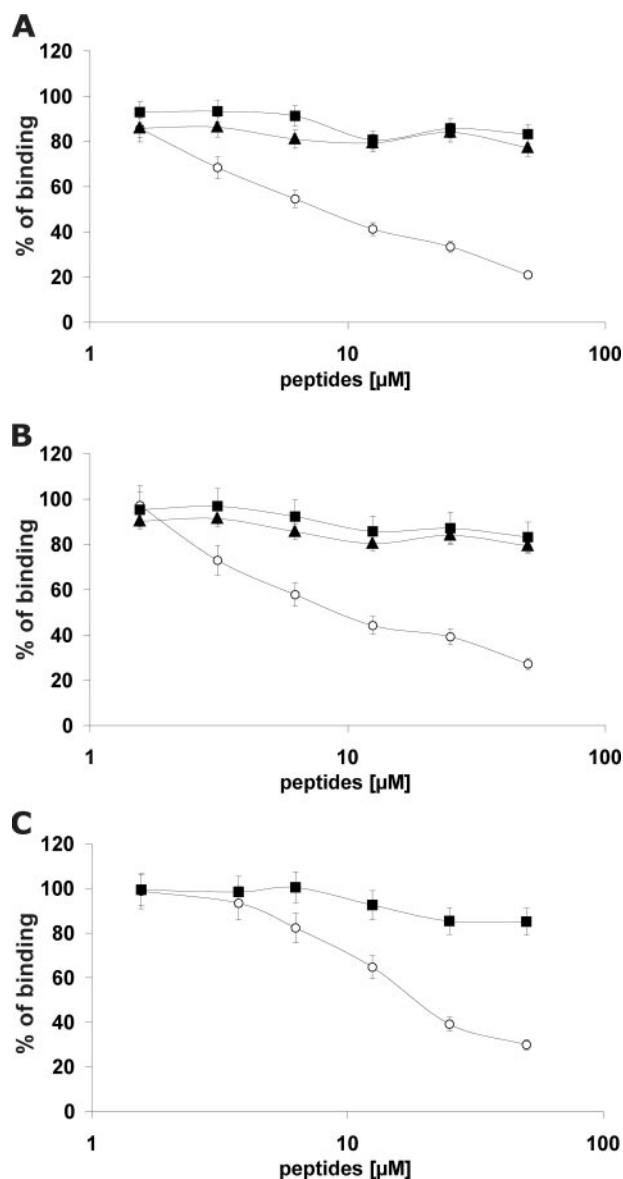


FIGURE 2. **Tetrameric peptide 4-23-5 inhibits the binding of VEGF family members with Flt-1 receptor.** *A–C*, dose-dependent inhibition of PlGF (*A*), VEGF-A (*B*), and VEGF-B (*C*) interaction with Flt-1 exerted by 4-23-5 peptide in competitive ELISA-based assays. Tetrameric 4-23-5 (○), 4-23-A (▲), and 21-1-5 (■) peptides were assayed at concentrations ranging between 1.56 and 50.0 μM. The results represent the average of three independent experiments. The error bars represent the S.D.

Inhibitory Properties of the Peptide 4-23-5—Because the binding mechanism of VEGFs members able to recognize Flt-1 is similar (18, 36–38), we first investigated whether 4-23-5 was capable to inhibit also the interactions of human VEGF-A and VEGF-B with Flt-1 receptor. The peptide was able to block in a dose-dependent fashion the interaction of VEGF-A (Fig. 2B) and VEGF-B (Fig. 2C) with Flt-1. In the first case, the IC₅₀ was similar to that observed for PlGF-Flt-1 interaction (about 10 μM), whereas for VEGF-B, the IC₅₀ was slightly higher (about 18 μM). Again, the control tetrameric peptides 21-1-5 and 4-23-A did not exhibit inhibition. Remarkably, the 4-23-5 peptide also blocked the interaction between human PlGF/VEGF heterodimer with Flt-1 and that of mouse PlGF or VEGF-A with the corresponding mouse receptor (not shown).

Anti-VEGFR-1 Peptide Modulates Angiogenesis

To evaluate the influence of the multimeric structure and the contribution from single residues on peptide activity, a panel of analogues was designed, synthesized (supplemental Table S3), and tested at the single 50 μM concentration in the PlGF/Flt-1 competition assay. All sequence (supplemental Fig. S2A) and structural (supplemental Fig. S2B) variants tested were ineffective or exhibited only a slight activity when compared with the parent 4-23-5 peptide used at 12.5 μM . These outcomes indicate that both the sequence and the multimeric structure of the 4-23-5 peptide are required for its inhibitory properties.

Binding Properties of the Peptide 4-23-5—The ability of selected peptide to inhibit the interaction of all three VEGF family members with Flt-1 receptor suggested that it seemingly interacts with the receptor. To validate this hypothesis, 4-23-5 or control peptides were coated on microtiter plates, and the binding of soluble growth factors or chimeric recombinant Fc/Flt-1 receptors was assessed by ELISA assays. Remarkably, VEGF-A and PlGF did not bind the immobilized peptide (not shown), whereas both human and mouse Flt-1 specifically interacted with the synthetic ligand (Fig. 3A) in a dose-dependent manner (supplemental Fig. S3). Moreover, PlGF and VEGF-A were both able to inhibit in a dose-dependent manner the binding of Flt-1 to coated 4-23-5 peptide, showing a 50% inhibition when used at 10-fold molar excess over Flt-1 concentration (Fig. 3B). Importantly, the peptide failed to bind KDR and Flk-1 receptors (Fig. 3C), demonstrating a strong selectivity for the high affinity receptor.

Stability and Neutralizing Properties of Peptide 4-23-5—Before starting cell-based assays, we verified the stability of 4-23-5 in serum over time. This tetrameric ligand, composed by unnatural amino acids, was essentially fully stable in 10% FBS for 7 days (168 h) (Fig. 4A). This experiment also proved that, under these conditions, the peptide did not bind serum proteins as no peptide subtraction by the precipitation of serum proteins performed before the HPLC analysis was observed (see “Experimental Procedures”).

The neutralizing activity of 4-23-5 peptide was initially evaluated in receptor phosphorylation assays. The peptide was able to reduce in a dose-dependent manner PlGF- and VEGF-induced phosphorylation of human Flt-1 in a cell line (293-Flt-1) (18) stably overexpressing the receptor (Fig. 4, B and C, respectively). Notably, when used at 4.0 μM , the peptide prevented the phosphorylation of more than 50%. At 20 μM , the efficacy increased and was similar to that obtained with a neutralizing anti-PlGF mAb (16D3, Thrombogenics, Leuven, Belgium) (Fig. 4B) or with neutralizing anti-VEGF antibodies (R&D Systems) (Fig. 4C) used at about 3 nM. The control peptide 21-1-5 used at 20 μM was ineffective in both experiments (Fig. 4, B and C). As expected on the basis of the ELISA data, the peptide was unable to interfere with the VEGF-A-induced KDR phosphorylation on HUVEC when used at 20 μM (Fig. 4D), confirming its high selectivity for Flt-1 over the lower affinity receptor (Fig. 3C).

Anti-angiogenic Activity of the 4-23-5 Peptide—The anti-angiogenic activity of the selected peptide was first assessed by testing its capability to suppress the induction of capillary-like tube formation (CTF), stimulated by PlGF or VEGF-A, of human primary endothelial cells (HUVEC) grown on Matrigel. HUVECs stimulated by PlGF (Fig. 5, A–G) or VEGF-A (Fig. 5,

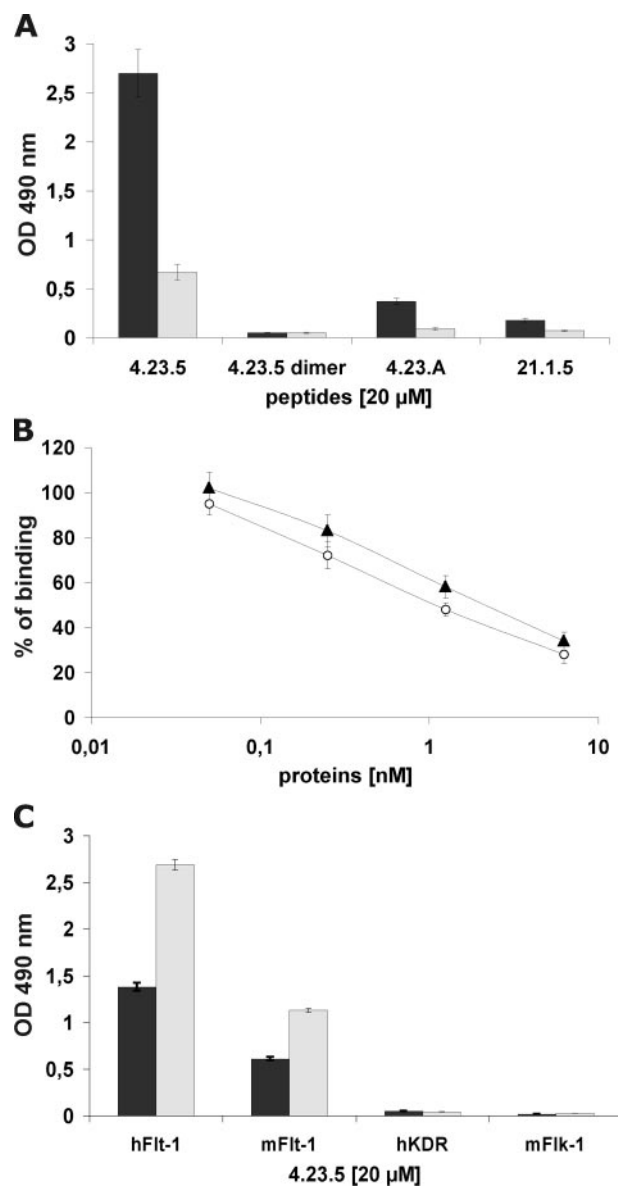


FIGURE 3. Tetrameric peptide 4-23-5 binds specifically to Flt-1 receptor. The binding properties of selected peptide were assessed by ELISA-based assays. *A*, binding of human (black bar) or mouse (gray bar) Flt-1 receptors (250 pM) to 4-23-5 peptide coated on a microtiter plate at 20 μM . The two receptors failed to bind to three control peptides: 4-23-5 dimer, 4-23-A, and 21-1-5 coated at the same concentration. *B*, dose-dependent inhibition of Flt-1 (125 pM) interaction with coated 4-23-5 peptide (20 μM) exerted by PlGF (○) and VEGF-A (▲). Soluble growth factors were assayed at concentrations ranging from 0.05 to 6.25 nM. *C*, dose-dependent interaction of human and mouse Flt-1 (hFlt-1 and mFlt-1) assayed at 125 pM (black bar) and 250 pM, (gray bar) with 4-23-5 peptide coated at 20 μM . VEGFRs-2 (human KDR (hKDR) and mouse Flk-1 (mFlk-1)) failed to bind 4-23-5 peptide in the same conditions. The results represent the average of three independent experiments. The error bars represent the S.D.

H–N) were able to generate structures similar to capillaries (Fig. 5, A and H). As shown in Fig. 5, B and I, the suppression of PlGF- and VEGF-A-induced CTF by 4-23-5 was virtually complete at 20 μM , whereas the control peptides 4-23-A and 21-1-5 were totally inactive even at 50 μM (Fig. 5, C and J and D and K, respectively). 4-23-5 was also tested at 4.0, 0.80, and 0.16 μM (Fig. 5, E, L, F, and M and G and N, respectively), showing again a complete inhibition at 4.0 μM . At 0.80 μM , CTF was only

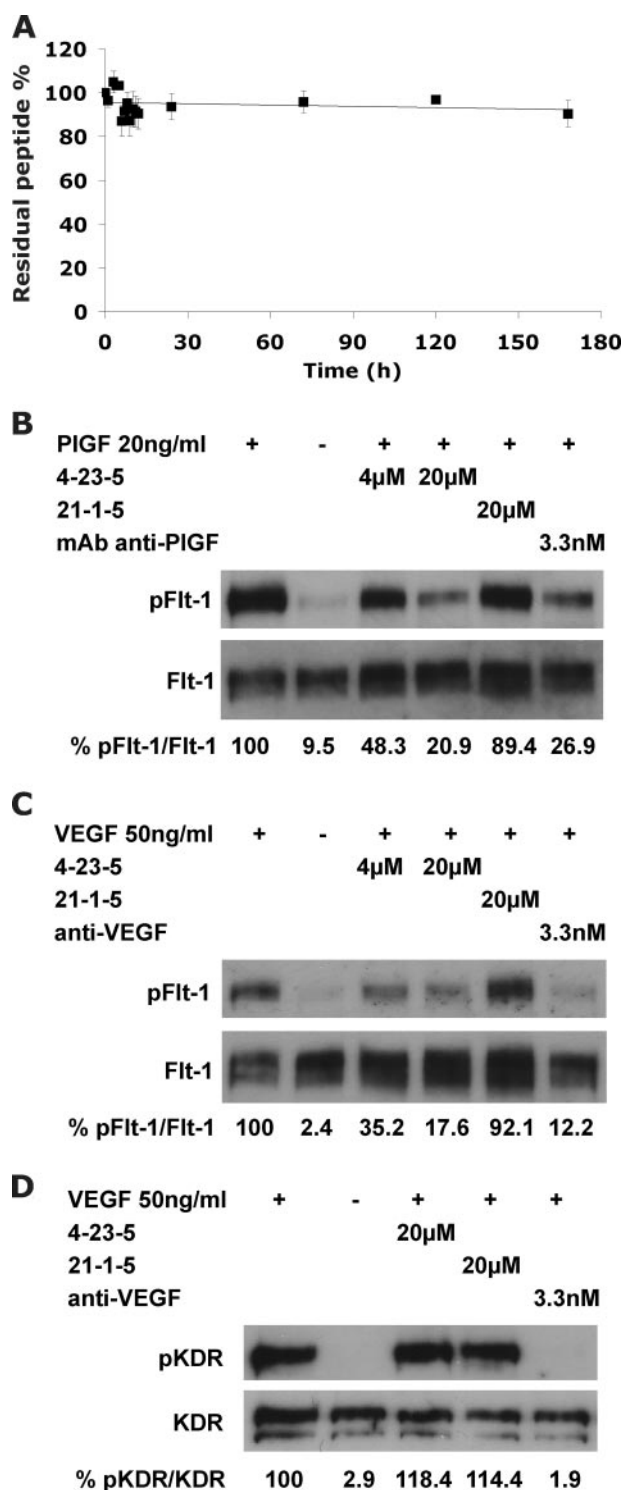


FIGURE 4. Stability and neutralizing properties of peptide 4-23-5. *A*, the resistance to enzyme degradation of the selected peptide was assessed by incubation in 10% fetal calf serum for 168 h. At time 0, after every hour within the first 12 h, and at 24, 72, 120, and 168 h, three aliquots were removed, centrifuged to remove proteins, and analyzed by HPLC (10 μ l, 1 μ g). Residual peptide quantity, expressed as the percentage of the initial amount *versus* time, was plotted. The results represent the average of three independent experiments. The *error bars* represent the S.D. The ability of selected peptide to inhibit the VEGFRs activation exerted by PIGF and VEGF-A was evaluated in receptor phosphorylation assays (*B–D*). Starved 293-hFlt1 cells were stimulated with 20 ng/ml PIGF (*B*) or 50 ng/ml of VEGF-A (*C*) for 10 min, in the presence or absence of active and control peptides. As controls, neutralizing anti-PIGF or anti-VEGF antibodies were used. Similarly, starved HUVECs were stimulated with VEGF-A (*D*). 100 μ g of cell lysate were used for Western blot

partially suppressed, whereas at the lowest concentration, the inhibition activity was essentially lost.

The anti-angiogenic activity of the peptide was confirmed in the *in vivo* model of the CAM assay (32). Alginate beads adsorbed with VEGF-A or PIGF alone or added with peptides were implanted on the top of 11-day-old chick embryo CAMs. VEGF-A (Fig. 6*A*) and PIGF (Fig. 6*B*) exerted a potent angiogenic response when compared with beads adsorbed with vehicle or peptides alone (Fig. 6*A*).

The addition of 4-23-5 peptide significantly inhibited the angiogenic response stimulated by either PIGF or VEGF-A in a dose-dependent manner in all the embryos tested. In contrast, no inhibition was elicited by the control peptide 21-1-5, except for a partial inhibition observed only in 2 out of the 6 embryos stimulated with VEGF-A and treated with 0.25 nmol of the control peptide (Fig. 6, and for representative pictures, see supplemental Fig. S4).

Peptide 4-23-5 Stimulates Corneal Neoangiogenesis—The molecular mechanism responsible for corneal avascularity has been recently elucidated (26). Corneal avascularity is maintained by the abundant expression of sFlt-1 and by the concomitant absence of full-length Flt-1. Indeed, although it is avascular, the cornea expresses VEGF-A, whose activity is prevented by sFlt-1. These findings make the cornea an ideal platform to assess the *in vivo* activity of neutralizing anti-Flt-1 molecules because, as reported previously, injection in the cornea of molecules able to displace VEGF from sFlt-1, such as anti-Flt-1 antibodies or PIGF, should induce spontaneous CNV (26). The injection of 20 nmol of peptide potently induced CNV (Fig. 7, *C* and *G*). The effect was also dose-dependent because injection of 4.0 nmol (Fig. 7, *B* and *F*) or 0.40 nmol (Fig. 7, *A* and *E*) still produced clearly visible effects, although to a reduced extent. Conversely, the injection of 20 nmol of control peptide 21-1-5 was unable to induce CNV (Fig. 7, *D* and *H*). Interestingly, the immunofluorescence analysis of cornea reported in Fig. 7*G* showed that after injection of the highest dosage of peptide, the formation of lymphatic vessels (red LYVE-1-positive vessels) was observable. Of utmost importance, a single injection of 4-23-5 produced a sustained effect detectable up to 7 days, in agreement with the high peptide stability observed *in vitro* (Fig. 4*A*).

DISCUSSION

Current strategies to block receptor tyrosine kinase activity are based on neutralization of natural ligands interaction or on inhibition of tyrosine kinase activity. Due to the high specificity and affinity, mAbs represent the primary approach for ligand neutralization. However, synthetic molecules still offer numerous advantages over biotherapeutics as they can be more easily

analyses. Anti-phospho-Flt-1 (*pFlt-1*) or anti-phospho-KDR (*pKDR*) antibodies were used to detect the level of receptor phosphorylation, whereas anti-Flt-1 (*Flt-1*) or anti-KDR (*KDR*) antibodies were used for normalization. The values of densitometry analyses, performed using ImageQuant 5.2 software (GE Healthcare) are shown. Values (in percentages) were calculated as the ratio of degree of receptor phosphorylation with respect to the total receptor amounts. The value of 100 has been arbitrarily assigned to PIGF- or VEGF-induced samples.

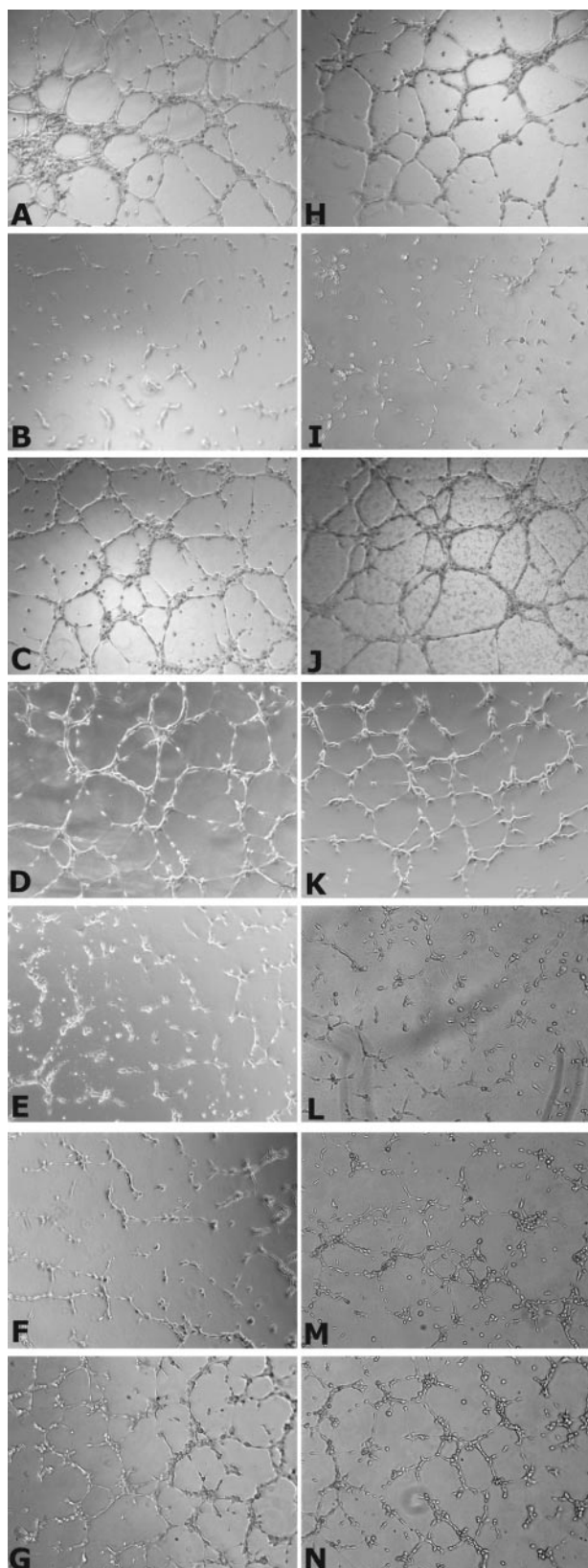


FIGURE 5. Tetrameric tripeptide 4-23-5 inhibits capillary-like tube formation induced by PIGF or VEGF-A. A–N, representative pictures of capillary-like tube formation stimulated with 100 ng/ml PIGF (A–G) or VEGF-A (H–N) in the presence or absence of active and control peptides. PIGF (A) or VEGF-A (H) in endothelial basal medium (EBM-2) was able to stimulate the formation of structure similar to capillaries. 4-23-5 peptide at 20 μ M completely prevented CTF induced by PIGF (B) or VEGF-A (I), whereas control peptides 4-23-A (C and

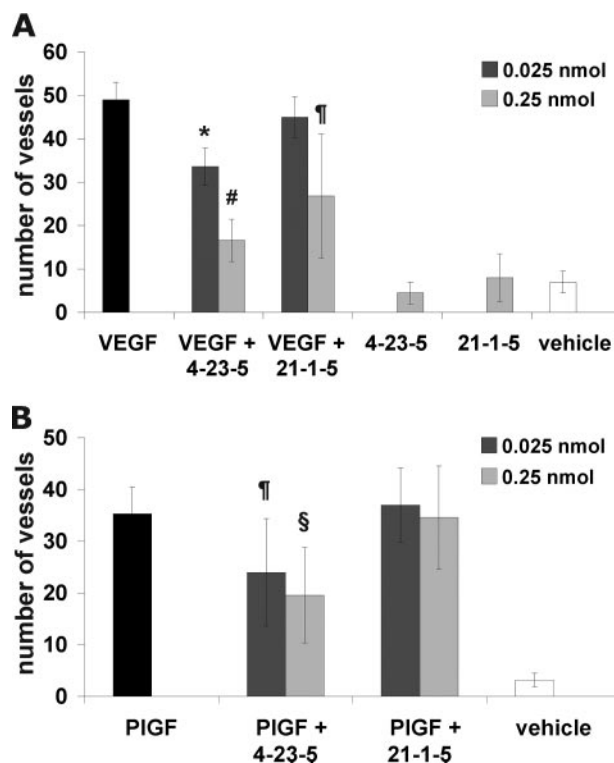


FIGURE 6. Tetrameric tripeptide 4-23-5 inhibits *in vivo* neovessels formation stimulated by VEGF-A or PIGF in CAM assay. A and B, alginate beads containing 150 ng/embryo of VEGF-A (A) or 250 ng/embryo of PIGF (B), with or without peptides, vehicle, or peptides alone, were placed on top of the CAM of fertilized White Leghorn chicken eggs at day 11 of incubation (6–8 eggs per experimental group). After 72 h, new blood vessels converging toward the implant were counted by two observers in a double-blind fashion under a stereomicroscope. Black bars, VEGF-A or PIGF; light gray bars, factors plus 0.25 nmol of peptides or peptides alone; dark gray bars, factors plus 0.025 nmol of peptide; white bars, vehicle. 4-23-5 peptide significantly inhibited either PIGF-induced or VEGF-A-induced angiogenesis in a dose-dependent manner in all the embryos tested. No inhibition was detected with the control peptide 21-1-5, except for a partial inhibition observed only in 2 out of the 6 embryos stimulated with VEGF-A and treated with 0.25 nmol of the control peptide. The error bars represent the S.D. *, $p < 0.005$ versus VEGF-A; #, $p < 0.0001$ versus VEGF-A; †, $p < 0.05$ versus VEGF-A or PIGF; §, $p < 0.005$ versus PIGF.

and cheaply produced, are more stable, and are generally free of contaminants of biological origin. Furthermore, they offer more opportunity for delivery.

In this perspective, we undertook a screening of combinatorial peptide libraries to search for antagonists of the VEGF high affinity receptor, which controls a variety of biological functions associated with pathological conditions (7). We report here the identification of a synthetic tetrameric tripeptide that binds to Flt-1 and prevents its interaction with all members of VEGF family able to recognize it (Fig. 2). The peptide has been selected from a library made with unnatural amino acids and screened by a competitive ELISA-based assay. Tetrameric structures based on branched polylysine were chosen to assemble random sequences as they reportedly increase the avidity of peptides for their targets (39) and, at the same time, enhance

(J) and 21-1-5 (D and K) at 50 μ M failed to block CTF. Tetrameric peptide 4-23-5 was still able to fully block CTF stimulated by both PIGF and VEGF-A at 4.0 μ M (E and L). At 0.80 μ M (F and M), a partial inhibitory effect was still present, whereas at 0.16 μ M (G and N), peptide lost the capability to inhibit CTF (original magnification $\times 10$).

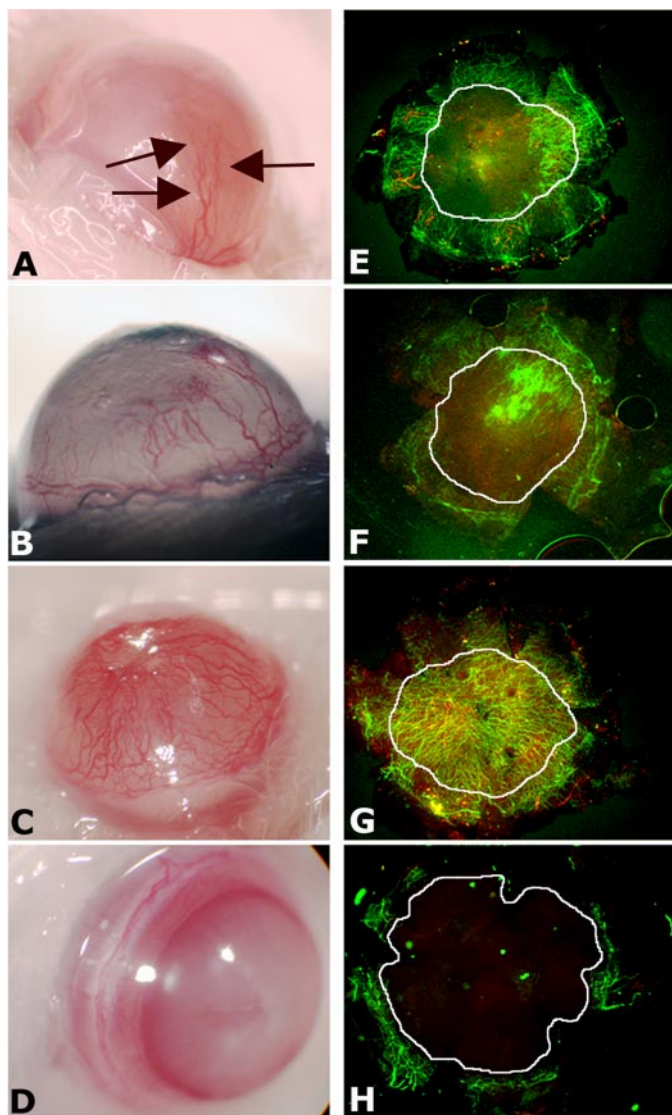


FIGURE 7. Tetrameric tripeptide 4-23-5 stimulates corneal neovascularization. A total of 0.4 (A and E), 4.0 (B and F), or 20.0 (C and G) nmol of 4-23-5 peptide and 20.0 nmol of control peptide 21-1-5 (D and H), in the same volume of DMSO, were injected in the corneas of BALB/c mice. After 7 days, corneas were photographed (A–D) and then harvested and flat-mounted. In A, new vessels are indicated with arrows. New vessels were immunostained (E–H) using anti-mouse CD31 antibodies (green) and anti-mouse-LYVE-1 antibodies (red). The areas corresponding to cornea have been indicated with a white circle. Blood vessels were defined as CD31-positive and LYVE-1-negative (original magnification $\times 4$).

the resistance to degradation by proteolytic enzymes (30). The use of unnatural amino acids further improves the stability of the resulting molecules, and indeed, the selected ligand shows an outstanding resistance in 10% serum (Fig. 4A) when compared with other recently reported anti-Flt-1 peptides (40–42). This property can be of particular interest in view of potential therapeutic applications.

The 4-23-5 peptide, despite the apparent low receptor affinity (around 10 μM), displays a high binding specificity for VEGFR-1, as demonstrated both in ELISA (Fig. 3C) and in receptor phosphorylation (Fig. 4, B–D) assays. Despite the sequence and structural similarity between the two VEGF receptors, the selected peptide appears incapable to interact with VEGFR-2. The anti-angiogenic activity of the 4-23-5 pep-

tide has been demonstrated using two of the most common angiogenic assays, the CTF and the CAM neovascularization assays and, in both experimental approaches, it is able to prevent the pro-angiogenic activity stimulated by PIGF or VEGF-A.

Notably, suppression of CTF stimulated by PIGF or VEGF (Fig. 5) demonstrates that the neutralization of ligand binding to Flt-1, and thus the block of the downstream receptor signaling, is sufficient alone to prevent all the biological events integral to the CTF process, such as cell proliferation, migration, and differentiation. In the same manner, the 4-23-5 peptide is capable to strongly inhibit in a dose-dependent way PIGF- and VEGF-induced CAM neovascularization (Fig. 6 and supplemental Fig. S4). The inhibition of CTF and neovascularization of CAM induced by PIGF was expected, due to the ability of PIGF to exclusively bind to Flt-1 receptor.

Remarkably, the observed complete blocking of VEGF-A-induced CTF together with the strong inhibition of VEGF-induced angiogenesis in the CAM assay exerted by 4-23-5 indicates that, despite the presence of both VEGFRs, *in vitro* and *in vivo* angiogenic response to VEGF stimulation can be abrogated by selective inhibition of the high affinity receptor alone (7, 40, 41). This result is supported by very recent data that demonstrated how the activation of Flt-1 is crucial for a correct stimulation of ECs by VEGF (19). Permanent inhibition of Flt-1 expression by RNA interference (using small interfering RNA) inhibited VEGF-A-induced HUVEC proliferation and CTF, with an extent higher than that obtained with permanent inhibition of KDR expression. Moreover, the deletion of Flt-1 induced a reduction of cell lifespan and an increase of cell senescence via p53/p21-dependent pathways, whereas that of KDR inhibited cell survival. In addition, it has been demonstrated that *in vivo*, the dosage of Flt-1 is crucial because recovery from hind limb ischemia was impaired in heterozygous *flt-1*^{+/-} mice. Interestingly, although it was previously reported that Flt-1 is able to interact with phosphatidylinositol 3-kinase (43), in both *in vitro* and *in vivo* approaches, the authors found that the total or the partial absence of Flt-1 leads to an increase of Akt activation by VEGF via VEGFR-2. The ability of VEGF to stimulate phosphatidylinositol 3/Akt pathway and cell survival via VEGFR-2 was already known (44). Interestingly the angiogenic impairment observed in *flt-1*^{+/-} mice was annulled in double heterozygous *flt-1*^{+/-} *akt*^{+/-} mice, in agreement with previous findings demonstrating that *akt*^{-/-} mice showed an augmented angiogenic response (45).

The specific and dose-dependent block of Flt-1 by 4-23-5 peptide may thus mimic the effect observed with small interfering RNA and was sufficient to inhibit both VEGF-dependent angiogenesis in CTF (Fig. 5) and neovascularization of CAM (Fig. 6). The strong effect we observe in the CAM assay after 72 h from the stimulus was probably due both to cell proliferation inhibition and to cell lifespan reduction, facilitated by the high stability of the peptide that allows a sustained inhibitory effect over the time. It should be considered also that the block of Flt-1 activation prevents possible cross-talk between the two receptors (46, 47) other than VEGF-induced receptors heterodimerization, whose role has not yet been fully elucidated.

Anti-VEGFR-1 Peptide Modulates Angiogenesis

The dose-dependent stimulation of CNV observed after peptide injection (Fig. 7) was similar to that previously obtained with neutralizing anti-Flt-1 antibodies or with small interfering RNA inhibition of sFlt-1 (26), suggesting that 4-23-5 peptide is able to displace the VEGF-A-sFlt-1 complex present in the cornea in physiological conditions, increasing the availability of VEGF-A for the stimulation of CNV. The similarity of the effects obtained with the specific anti Flt-1 reagents previously utilized and those induced with 4-23-5 peptide strongly suggests, as already demonstrated in ELISA and receptor phosphorylation assays, that the selected peptide has an elevated selectivity for Flt-1 also *in vivo*. Moreover, the absence of full-length Flt-1 receptor in the cornea suggests that VEGF-VEGFR2 interaction is crucial for the CNV, again supporting the view that the 4-23-5 peptide does not recognize VEGFR-2. This was also corroborated by the observation that at the highest peptide concentration injected in the cornea, the formation of new lymphatic vessels was evident (Fig. 7G), a result consistent with recent data on the ability of VEGF-A to also stimulate lymphangiogenesis and with findings indicating that the VEGF-VEGFR-2 interaction is crucial for this process (48). However, due to the peculiarity of this compartment, we cannot rule out that the observed CNV might also be due to other additional unknown or not well characterized mechanisms, such as preventing the ability of sFlt-1 to inhibit the activity of VEGF receptors by dimerization with their membrane bound forms (25).

Collectively, our results suggest that the peptide 4-23-5 is a new specific anti-Flt-1 compound with potential applications for molecular therapeutic approaches of pathologies in which angiogenesis and inflammation represent critical events.

Acknowledgments—We thank Prof. D. Collen, Chairman of the D. Collen Research Foundation, for support. We also thank V. Mercadante, M. Nozaki, and K. Yamada for technical assistance.

REFERENCES

1. Yancopoulos, G. D., Davis, S., Gale, N. W., Rudge, J. S., Wiegand, S. J., and Holash, J. (2000) *Nature* **407**, 242–248
2. Olsson, A. K., Dimberg, A., Kreuger, J., and Claesson-Welsh, L. (2006) *Nat. Rev. Mol. Cell Biol.* **7**, 359–371
3. Carmeliet, P. (2005) *Nature* **438**, 932–936
4. Ferrara, N., and Kerbel, R. S. (2005) *Nature* **438**, 967–974
5. De Falco, S., Gigante, B., and Persico, M. G. (2002) *Trends Cardiovasc. Med.* **12**, 241–246
6. Shibuya, M. (2006) *Angiogenesis* **9**, 225–230; discussion 231
7. Luttun, A., Tjwa, M., and Carmeliet, P. (2002) *Ann. N. Y. Acad. Sci.* **979**, 80–93
8. Kaplan, R. N., Rafii, S., and Lyden, D. (2006) *Cancer Res.* **66**, 11089–11093
9. Carmeliet, P., Moons, L., Luttun, A., Vincenti, V., Compernelle, V., De Mol, M., Wu, Y., Bono, F., Devy, L., Beck, H., Scholz, D., Acker, T., Di-Palma, T., Dewerchin, M., Noel, A., Stalmans, I., Barra, A., Blacher, S., Vandendriessche, T., Ponten, A., Eriksson, U., Plate, K. H., Foidart, J. M., Schaper, W., Charnock-Jones, D. S., Hicklin, D. J., Herbert, J. M., Collen, D., and Persico, M. G. (2001) *Nat. Med.* **7**, 575–583
10. Bellomo, D., Headrick, J. P., Silins, G. U., Paterson, C. A., Thomas, P. S., Gartside, M., Mould, A., Cahill, M. M., Tonks, I. D., Grimmond, S. M., Townson, S., Wells, C., Little, M., Cummings, M. C., Hayward, N. K., and Kay, G. F. (2000) *Circ. Res.* **86**, E29–35
11. Hiratsuka, S., Minowa, O., Kuno, J., Noda, T., and Shibuya, M. (1998) *Proc. Natl. Acad. Sci. U. S. A.* **95**, 9349–9354
12. Lyden, D., Hattori, K., Dias, S., Costa, C., Blaikie, P., Butros, L., Chadburn, A., Heissig, B., Marks, W., Witte, L., Wu, Y., Hicklin, D., Zhu, Z., Hackett, N. R., Crystal, R. G., Moore, M. A., Hajjar, K. A., Manova, K., Benezra, R., and Rafii, S. (2001) *Nat. Med.* **7**, 1194–1201
13. Rakic, J. M., Lambert, V., Devy, L., Luttun, A., Carmeliet, P., Claes, C., Nguyen, L., Foidart, J. M., Noel, A., and Munaut, C. (2003) *Investig. Ophthalmol. Vis. Sci.* **44**, 3186–3193
14. Wu, Y., Zhong, Z., Huber, J., Bassi, R., Finnerty, B., Corcoran, E., Li, H., Navarro, E., Balderes, P., Jimenez, X., Koo, H., Mangalampalli, V. R., Ludwig, D. L., Tonra, J. R., and Hicklin, D. J. (2006) *Clin. Cancer Res.* **12**, 6573–6584
15. Fischer, C., Jonckx, B., Mazzone, M., Zacchigna, S., Loges, S., Pattarini, L., Chorianopoulos, E., Liesenborghs, L., Koch, M., De Mol, M., Autiero, M., Wyns, S., Plaisance, S., Moons, L., van Rooijen, N., Giacca, M., Stassen, J. M., Dewerchin, M., Collen, D., and Carmeliet, P. (2007) *Cell* **131**, 463–475
16. Wang, H., and Keiser, J. A. (1998) *Circ. Res.* **83**, 832–840
17. Barleon, B., Sozzani, S., Zhou, D., Weich, H. A., Mantovani, A., and Marme, D. (1996) *Blood* **87**, 3336–3343
18. Errico, M., Riccioni, T., Iyer, S., Pisano, C., Acharya, K. R., Persico, M. G., and De Falco, S. (2004) *J. Biol. Chem.* **279**, 43929–43939
19. Nishi, J., Minamino, T., Miyauchi, H., Nojima, A., Tateno, K., Okada, S., Orimo, M., Moriya, J., Fong, G. H., Sunagawa, K., Shibuya, M., and Komuro, I. (2008) *Circ. Res.* **103**, 261–268
20. Clauss, M., Weich, H., Breier, G., Knies, U., Rockl, W., Waltenberger, J., and Risau, W. (1996) *J. Biol. Chem.* **271**, 17629–17634
21. Sawano, A., Iwai, S., Sakurai, Y., Ito, M., Shitara, K., Nakahata, T., and Shibuya, M. (2001) *Blood* **97**, 785–791
22. Luttun, A., Tjwa, M., Moons, L., Wu, Y., Angelillo-Scherrer, A., Liao, F., Nagy, J. A., Hooper, A., Priller, J., De Klerck, B., Compernelle, V., Daci, E., Bohlen, P., Dewerchin, M., Herbert, J. M., Fava, R., Matthys, P., Carmeliet, G., Collen, D., Dvorak, H. F., Hicklin, D. J., and Carmeliet, P. (2002) *Nat. Med.* **8**, 831–840
23. Hattori, K., Heissig, B., Wu, Y., Dias, S., Tejada, R., Ferris, B., Hicklin, D. J., Zhu, Z., Bohlen, P., Witte, L., Hendrikx, J., Hackett, N. R., Crystal, R. G., Moore, M. A., Werb, Z., Lyden, D., and Rafii, S. (2002) *Nat. Med.* **8**, 841–849
24. Kaplan, R. N., Riba, R. D., Zacharoulis, S., Bramley, A. H., Vincent, L., Costa, C., MacDonald, D. D., Jin, D. K., Shido, K., Kerns, S. A., Zhu, Z., Hicklin, D., Wu, Y., Port, J. L., Altorki, N., Port, E. R., Ruggero, D., Shmelkov, S. V., Jensen, K. K., Rafii, S., and Lyden, D. (2005) *Nature* **438**, 820–827
25. Kendall, R. L., and Thomas, K. A. (1993) *Proc. Natl. Acad. Sci. U. S. A.* **90**, 10705–10709
26. Ambati, B. K., Nozaki, M., Singh, N., Takeda, A., Jani, P. D., Suthar, T., Albuquerque, R. J., Richter, E., Sakurai, E., Newcomb, M. T., Kleinman, M. E., Caldwell, R. B., Lin, Q., Ogura, Y., Orecchia, A., Samuelson, D. A., Agnew, D. W., St Leger, J., Green, W. R., Mahasreshti, P. J., Curiel, D. T., Kwan, D., Marsh, H., Ikeda, S., Leiper, L. J., Collinson, J. M., Bogdanovich, S., Khurana, T. S., Shibuya, M., Baldwin, M. E., Ferrara, N., Gerber, H. P., De Falco, S., Witt, J., Baffi, J. Z., Raisler, B. J., and Ambati, J. (2006) *Nature* **443**, 993–997
27. De Falco, S., Ruvoletto, M. G., Verdoliva, A., Ruvo, M., Raucchi, A., Marino, M., Senatore, S., Cassani, G., Alberti, A., Pontisso, P., and Fassina, G. (2001) *J. Biol. Chem.* **276**, 36613–36623
28. Marino, M., Ruvo, M., De Falco, S., and Fassina, G. (2000) *Nat. Biotechnol.* **18**, 735–739
29. Verdoliva, A., Marasco, D., De Capua, A., Saporito, A., Bellofiore, P., Manfredi, V., Fattorusso, R., Pedone, C., and Ruvo, M. (2005) *ChemBioChem* **6**, 1242–1253
30. Bracci, L., Falciani, C., Lelli, B., Lozzi, L., Runci, Y., Pini, A., De Montis, M. G., Tagliamonte, A., and Neri, P. (2003) *J. Biol. Chem.* **278**, 46590–46595
31. Fields, G. B., and Noble, R. L. (1990) *Int. J. Pept. Protein Res.* **35**, 161–214
32. Mitola, S., Belleri, M., Urbinati, C., Coltrini, D., Sparatore, B., Pedrazzi, M., Melloni, E., and Presta, M. (2006) *J. Immunol.* **176**, 12–15
33. Tam, J. P. (1988) *Proc. Natl. Acad. Sci. U. S. A.* **85**, 5409–5413
34. Furka, A., Sebastyen, F., Asgedom, M., and Dibo, G. (1991) *Int. J. Pept.*

- Protein Res.* **37**, 487–493
35. Lam, K. S., Salmon, S. E., Hersh, E. M., Hruby, V. J., Kazmierski, W. M., and Knapp, R. J. (1991) *Nature* **354**, 82–84
 36. Wiesmann, C., Fuh, G., Christinger, H. W., Eigenbrot, C., Wells, J. A., and de Vos, A. M. (1997) *Cell* **91**, 695–704
 37. Iyer, S., Leonidas, D. D., Swaminathan, G. J., Maglione, D., Battisti, M., Tucci, M., Persico, M. G., and Acharya, K. R. (2001) *J. Biol. Chem.* **276**, 12153–12161
 38. Iyer, S., Scotney, P. D., Nash, A. D., and Ravi Acharya, K. (2006) *J. Mol. Biol.* **359**, 76–85
 39. Fassina, G. (1992) *J. Chromatogr.* **591**, 99–106
 40. El-Mousawi, M., Tchistiakova, L., Yurchenko, L., Pietrzynski, G., Moreno, M., Stanimirovic, D., Ahmad, D., and Alakhov, V. (2003) *J. Biol. Chem.* **278**, 46681–46691
 41. Bae, D. G., Kim, T. D., Li, G., Yoon, W. H., and Chae, C. B. (2005) *Clin. Cancer Res.* **11**, 2651–2661
 42. Taylor, A. P., and Goldenberg, D. M. (2007) *Mol. Cancer Ther.* **6**, 524–531
 43. Cunningham, S. A., Waxham, M. N., Arrate, P. M., and Brock, T. A. (1995) *J. Biol. Chem.* **270**, 20254–20257
 44. Gerber, H. P., McMurtrey, A., Kowalski, J., Yan, M., Keyt, B. A., Dixit, V., and Ferrara, N. (1998) *J. Biol. Chem.* **273**, 30336–30343
 45. Chen, J., Somanath, P. R., Razorenova, O., Chen, W. S., Hay, N., Bornstein, P., and Byzova, T. V. (2005) *Nat. Med.* **11**, 1188–1196
 46. Autiero, M., Waltenberger, J., Communi, D., Kranz, A., Moons, L., Lambrechts, D., Kroll, J., Plaisance, S., De Mol, M., Bono, F., Kliche, S., Fellbrich, G., Ballmer-Hofer, K., Maglione, D., Mayr-Beyrle, U., Dewersch, M., Dombrowski, S., Stanimirovic, D., Van Hummelen, P., Dehio, C., Hicklin, D. J., Persico, G., Herbert, J. M., Communi, D., Shibuya, M., Colten, D., Conway, E. M., and Carmeliet, P. (2003) *Nat. Med.* **9**, 936–943
 47. Neagoe, P. E., Lemieux, C., and Sirois, M. G. (2005) *J. Biol. Chem.* **280**, 9904–9912
 48. Nagy, J. A., Vasile, E., Feng, D., Sundberg, C., Brown, L. F., Detmar, M. J., Lawitts, J. A., Benjamin, L., Tan, X., Manseau, E. J., Dvorak, A. M., and Dvorak, H. F. (2002) *J. Exp. Med.* **196**, 1497–1506